Nonreciprocal Solar Thermophotovoltaics

Sina Jafari Ghalekohneh and Bo Zhao*
Department of Mechanical Engineering, University of Houston, Houston, Texas 77204, USA

(Received 26 April 2022; revised 12 July 2022; accepted 23 August 2022; published 29 September 2022)

This paper is a contribution to the Physical Review Applied collection titled Photovoltaic Energy Conversion.

Traditional solar thermophotovoltaics (STPVs) rely on an intermediate layer to tailor sunlight for better efficiencies. However, the thermodynamic efficiency limit of STPVs, which has long been understood to be the blackbody limit (85.4%), is still far lower than the Landsberg limit (93.3%), the ultimate efficiency limit for solar energy harvesting. In this work, we show that the efficiency deficit is caused by the inevitable back emission of the intermediate layer towards the sun resulting from the reciprocity of the system. We hereby propose nonreciprocal solar theromophotovoltaics (NSTPV) that utilize an intermediate layer with nonreciprocal radiative properties. Such a nonreciprocal intermediate layer can substantially suppress its back emission to the sun and funnel more photon flux towards the cell. We show that, with such improvement, the NSTPV system can reach the Landsberg limit, and practical NSTPV systems with single-junction photovoltaic cells can also experience a significant efficiency boost.

DOI: 10.1103/PhysRevApplied.18.034083

I. INTRODUCTION

As a popular way to harvest solar energy, solar cells play an important role in achieving energy sustainability and security. Typical solar cells, however, use only the part of the solar spectrum that is above the band gap of the cell to produce electricity. Such restriction constrains the efficiency of single-junction solar cells to the well-known Shockley-Queisser (SQ) limit (40.7%) for fully concentrated sunlight [1]. Meanwhile, solar cell power generation is restricted to only the daytime. Solar thermophotovoltaic (STPV) systems offer a solution to utilizing the full solar spectrum for 24/7 power generation. As shown in Fig. 1(a), an STPV system utilizes an intermediate layer between the sun and the STPV cell. The front side of the intermediate layer, i.e., the side facing the sun, is designed to absorb all photons coming from the sun. In this way, the solar energy is converted to the thermal energy of the intermediate layer and elevates the temperature of the intermediate layer. The backside of the intermediate layer is designed such that it only emits photons that have higher energy than the band gap of the STPV cell. In doing so, the STPV can harvest the full spectrum of solar radiation, and its thermodynamic limit has been shown to be the blackbody limit (85.4%) [2]. Besides the improved efficiency, STPVs promise compactness and dispatchability compared to traditional solar cells. As one of the important application scenarios, STPVs can be coupled with an economical thermal energy storage unit [3,4] and generate electricity 24/7. With the efficiency of thermophotovoltaics reaching 40%, STPVs become competitive with combined cycle turbines from both efficiency and economic standpoints [5–7]. Because of these attractive advantages and promises, STPVs have drawn tremendous attention in both small- and large-scale power production systems [8–10].

Despite the significant efficiency advantages over solar cells, traditional STPVs still have detrimental irreversibility or exergy destruction. This is because the intermediate layer in conventional STPVs is a reciprocal optical component, in which Kirchhoff's law of thermal radiation is valid [7,11–13]. Therefore, the emissivity and absorptivity are always equal for a given direction, polarization, and frequency. Reciprocity guarantees that, while the intermediate layer is receiving the sunlight, there is unavoidable thermal emission from the front side of the intermediate layer towards the sun, as shown by the arrows on top of the emitter in Fig. 1(a). Such back emission is intrinsic to the system and cannot be eliminated by spectral control of the emissivity of the absorber [14,15]. Since the emission towards the sun cannot be harvested and essentially is lost, this back emission represents a primary intrinsic loss mechanism, especially considering that the temperature of the intermediate layer can reach 2000 K or even higher [16].

In this work, we propose a nonreciprocal [17–21] solar thermophotovoltaic (NSTPV) system that can eliminate the back emission of the intermediate layer towards the sun, as depicted in Fig. 1(b). In this system, the intermediate layer is designed to be nonreciprocal so that it can absorb from the front side but emit only to the backside [21]. We show that such a system allows all emissions from the intermediate layer to be directed to the cell,

*bzhao8@uh.edu

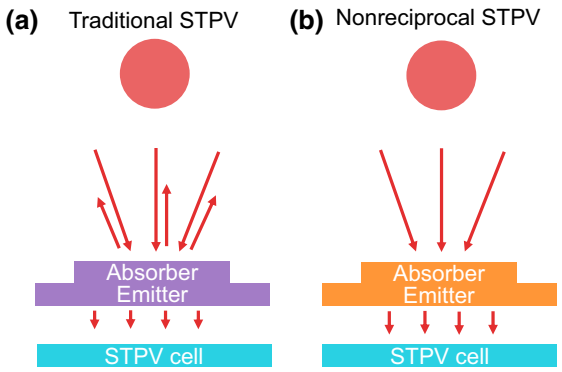

FIG. 1. (a) Illustration of traditional STPV and (b) nonreciprocal STPV. The absorber of traditional STPV has back radiation towards the sun. In nonreciprocal STPV, the back emission from the intermediate layer is suppressed, and more incoming energy is directed towards the cell. The nonreciprocal behavior of the intermediate layer can be made wavelength selective.

leading to a higher photon flux to the thermophotovoltaic cell and generating more electric power. From a thermodynamic analysis, we show that the ultimate efficiency of NSTPV is the Landsberg limit, significantly higher than the blackbody limit for traditional STPV systems. We note it has been shown that nonreciprocity is required to reach the Landsberg limit [22], as elaborated in previous designs with Landsberg efficiency [23, 24]. However, in stark contrast to previously proposed deigns, which require multiple nonreciprocal components to improve efficiency appreciably, our NSTPV requires only one nonreciprocal intermediate layer to trigger significant efficiency benefits and can be easily coupled to thermal energy storage units, representing a unique design with both theoretical and practical advantages.

II. RESULTS AND DISCUSSION

The efficiency improvement is enabled by the nonreciprocal intermediate layer, whose functionality is depicted in Fig. 2(a). The front side of the nonreciprocal intermediate layer can perfectly absorb the incident energy (absorptivity $\alpha = 1$) but has zero emissivity. The emission is rerouted to the backside, resulting in the emissivity of the backside of the structure being unity ($\varepsilon = 1$). With these radiative properties, thermodynamics requires that the incident energy from the backside is perfectly transmitted through the structure (transmissivity $t = 1$). Such nonreciprocal radiative properties have been recently proposed and proven to be possible [21]. The nonreciprocal intermediate layer here is in fact acting like a three-port heat circulator with one of the ports coupled with a blackbody. Together they can absorb energy from the sun but redirect the energy in the direction of the converter, as shown in Fig. 2(a). The benefit of this layer can be illustrated in the thermodynamic analysis of the efficiencies of STPV systems.

A. Ultimate efficiency of reciprocal STPVs

We start by revisiting the traditional STPV systems and show how the system can be improved with the nonreciprocal intermediate layer. As we intend to find the theoretical limit of the STPV, we consider the full concentration of the incoming solar radiation. In reciprocal STPV systems shown in Fig. 2(b), the input energy from the sun, E_s, carries an entropy flux $S_s = (4/3)E_s/T_s$, where $E_s = \sigma T_s^4$ with σ the Stefan-Boltzmann constant and T_s the temperature of the sun [2]. Since the intermediate layer is reciprocal, there is an energy flow $E_b = \sigma T_l^4$ emitted from the front side of the intermediate layer back towards the sun. Here, T_l is the temperature of the intermediate layer. The associated entropy flux is $S_b = (4/3)E_b/T_l$. S_g is the generated entropy due to the absorption and emission process at the front surface of the intermediate layer, which is given by [2,25,26]

$$S_g = E_s\left(\frac{1}{T_l} - \frac{4}{3T_s}\right) + \frac{1}{3}\frac{E_b}{T_l}. \tag{1}$$

In the above equation, the first term is the generated entropy due to absorption, and the second term is due to emission. Heat flux from the intermediate layer is converted to work output P with a Carnot converter, and the heat flux rejected to the ambient and its associated entropy are respectively Q and Q/T_a, where T_a is the ambient temperature. From the energy and entropy balance, we obtain

$$E_s = E_b + Q + P, \tag{2}$$

and

$$S_s + S_g = \frac{Q}{T_a} + S_b. \tag{3}$$

The efficiency can be obtained as

$$\eta = \frac{P}{E_s} = \left(1 - \frac{T_a}{T_l}\right)\left[1 - \left(\frac{T_l}{T_s}\right)^4\right]. \tag{4}$$

We assume $T_a = 300$ K and $T_s = 6000$ K. Therefore, the above equation has its maximum value of 85.4% when $T_l = 2544$ K, which is the blackbody limit for traditional STPV systems.

B. Ultimate efficiency of nonreciprocal STPVs

In the proposed NSTPV system [Fig. 2(c)], the nonreciprocal intermediate layer can help eliminate the entropy production on the front side of the intermediate layer. Here we assume the nonreciprocal capability shown in Fig. 2(a) is achieved for all wavelengths. In this way, all photons from the sun can be passed to the converter

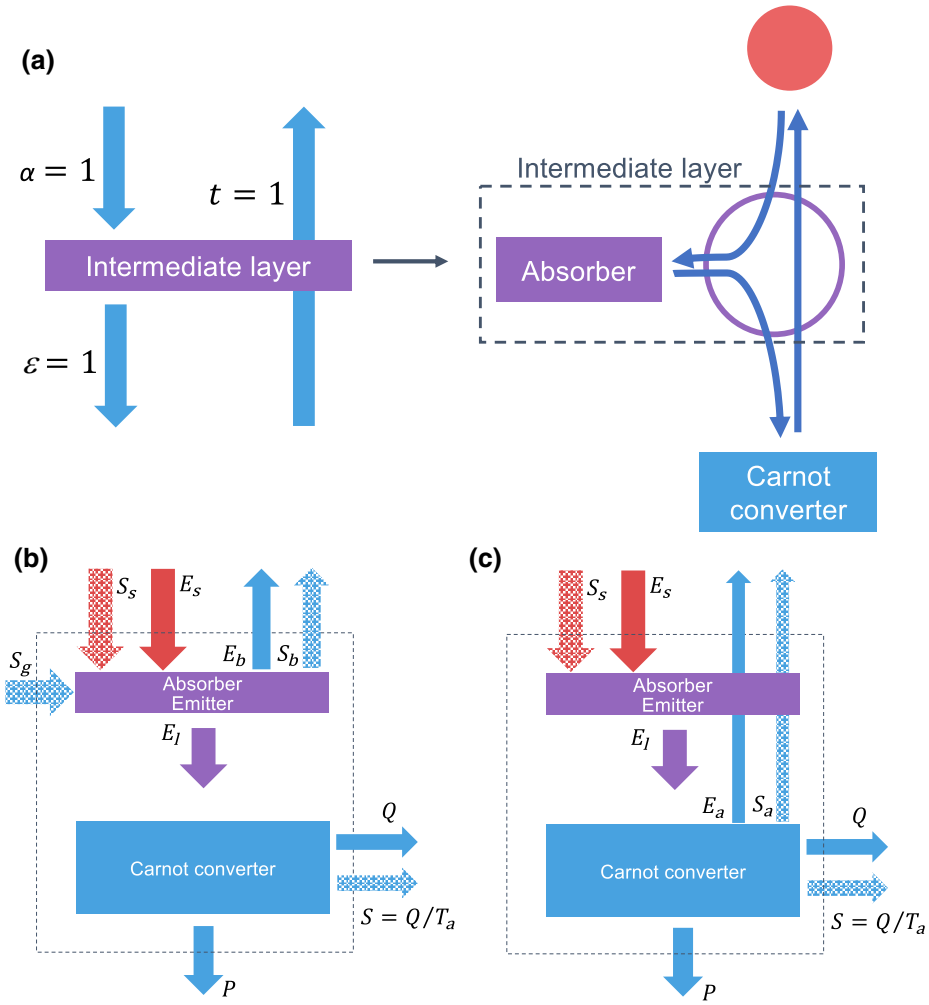

FIG. 2. (a) The functionality of the nonreciprocal intermediate layer as a circulator coupled to a blackbody emitter. The energy and entropy fluxes in ideal (b) reciprocal STPV, and (c) NSTPV systems.

through the intermediate layer. Meanwhile, in doing so, the incoming energy to the intermediate layer and the emitted energy from the backside (E_l) is exactly equivalent, i.e., $E_s = E_l$. Similar to the reciprocal STPV, here we consider the fully concentrated sunlight to find the limit of our NSTPV. Therefore, at this limit, based on the energy balance equation, the intermediate layer has the same temperature as the sun $T_l = T_s$, and the heat transfer between the sun and the intermediate layer echoes the scenario in Ref. [27] in which radiative heat flux is transferred between bodies with the same temperature. The entropy generation of the intermediate layer has a form similar to Eq. (1), $S_g = E_s((1/T_l) - (4/3)(1/T_s)) + (1/3)(E_l/T_l)$. Substituting $T_l = T_s$ and $E_l = E_s$, the generated entropy in the intermediate layer can be shown to be zero. As shown below, avoiding this entropy generation can significantly improve the efficiency of the system.

Since energy incident from the bottom part of the intermediate layer is perfectly transmitted, the radiated energy from the converter, E_a, with associated entropy $S_a = (4/3)E_a/T_a$, passes through the intermediate layer and leaves the system. Thus, the energy and entropy balance for the nonreciprocal system yield

$$E_s = E_a + Q + P, \tag{5}$$

and

$$S_s = \frac{Q}{T_a} + S_a. \tag{6}$$

Therefore, one obtains

$$\eta = \frac{P}{E_s} = 1 - \frac{4}{3}\frac{T_a}{T_s} + \frac{1}{3}\left(\frac{T_a}{T_s}\right)^4, \tag{7}$$

which is the Landsberg limit, 93.3%, and significantly higher than the blackbody limit of the traditional STPV system. We should note that Eq. (7) is obtained for the limiting case, where $T_l = T_s$. To reach the Landsberg

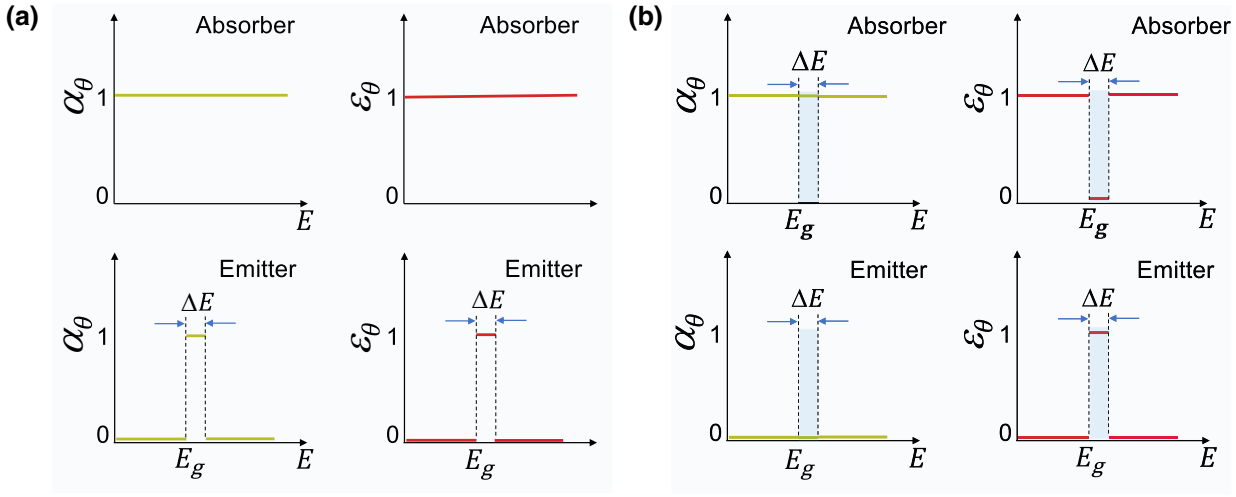

FIG. 3. Ideal spectral directional absorptivity (α_θ) and emissivity (ε_θ) of the intermediate layer in (a) reciprocal STPVs and (b) nonreciprocal STPVs. The nonreciprocal region is shaded in (b). We assume all directions possess the properties depicted in (a) for the reciprocal STPV system. For the absorber in the nonreciprocal system, the properties shown in (b) hold for all angles. For the emitter, the properties shown in (b) hold from the normal direction to θ_e, and beyond this angular range, the emitter has the same properties as the emitter in the reciprocal system.

efficiency in NSTPVs, one can adopt the convertor design proposed in Ref. [23] or [24] that can perform as Carnot converters for the purpose here. Compared to existing solar energy harvesting systems that can reach the Landsberg limit [2,23,24], the proposed NSTPV system represents a unique system that can straightforwardly couple with thermal storage units for power generation on demand. Therefore, similar to an STPV, it can be made scalable, compact, and dispatchable. The other unique advantage of the proposed NSTPV is that the efficiency improvement from nonreciprocity can be immediately appreciated by using just one nonreciprocal layer (the intermediate layer) when used with practically readily available single-junction cells, as we show in the following. This is in stark contrast to other systems [23,24] that generally require multiple nonreciprocal devices before the benefit of nonreciprocity becomes apparent.

C. Nonreciprocal STPVs with single-junction cells

In traditional STPVs with single-junction cells, an ideal intermediate layer should have broadband absorption on the front side shown in Fig. 3(a) to capture the fully concentrated sunlight. (We note that in the case of low concentrations, wavelength-selective absorbers can be beneficial [14,15]. Our following analysis and discussions, however, are valid regardless of the concentration.) On the backside of the intermediate layer, narrowband emission is preferred to radiate photons just above the band gap of the single-junction cell [28,29]. The narrowband emission from the emitter, however, needs to be compensated with an emitter with a much larger area than the absorber in order to balance the energy flow. In fact, reaching the ultimate efficiency requires an emitter with an infinitely large area [28]. For finite size, the desired emitter should have a high emissivity just above the band gap but with a certain bandwidth, as depicted in Fig. 3(a) [28,30,31]. Here, α_θ is the spectral directional absorptivity, ε_θ is the spectral directional emissivity, and E_g is the band gap energy. The radiative properties are assumed to be diffusive. We note that instead of engineering the radiative properties of the emitter, one can engineer the cell or use a filter in between the cell and the emitter to achieve the same wavelength selectivity [13,32–35]. The functionalities in terms of photon management are essentially the same as an emitter with properties as in Fig. 3(a), although specific methods can have practical advantages [13,33–35].

Based on the design rationale in the reciprocal STPV system, here we propose a wavelength-selective nonreciprocal intermediate layer with properties depicted in Fig. 3(b) for NSTPV systems with a single-junction cell. Within the frequency range just above the band gap, the intermediate layer possesses the nonreciprocal functionality depicted in Fig. 2(a). In this way, one allows useful photons to be emitted to the cell, and still have the benefit of suppressing the back emission of the absorber to the sun in this wavelength range. Outside this wavelength range, the spectral radiative properties are identical to the reciprocal case in Fig. 3(a). We keep the bandwidth of the nonreciprocal range ΔE as a parameter that can be optimized.

Besides the consideration of the spectral properties, there needs to be an additional consideration of the constraint in the angular range for the nonreciprocal radiative

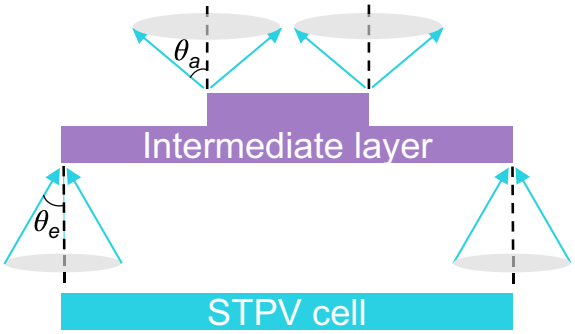

FIG. 4. The trade-off in spatial and angular concentration of rays due to the étendue conservation.

properties. Such constraint comes from the fact that the area of the emitter is larger than the absorber for the intermediate layer. Therefore, in the nonreciprocal frequency range ΔE, the back emission from the cell needs to transmit through the intermediate layer that has a changing cross-section area. In this case, the angular range of the transmitted beam is subject to the constraints from the brightness theorem or the étendue conservation [36–38]. As depicted in Fig. 4, the étendue occupied by the beam that is transmitted through the intermediate layer should be conserved.

For a light beam propagating through an area dA within a solid angle $d\Omega$ in a medium with refractive index n, its étendue can be expressed as $n^2 dA\cos\theta d\Omega$ [36,38], where θ is the polar angle and $d\Omega = \sin\theta d\theta d\phi$ with ϕ the azimuthal angle. Without losing generality, we consider a beam within a cone centered in the normal direction up to a certain polar angle. Its étendue is

$$\int_0^{2\pi}\int_0^{\theta} n^2 dA\cos\theta\,\sin\theta d\theta d\phi = \pi n^2 A\,\sin^2\theta. \tag{8}$$

In the proposed system, the incident medium and the transmitted medium are the same, and, therefore, the étendue conservation results in $A_e\sin^2\theta_e = A_a\sin^2\theta_a$, where A_e and A_a are the areas of the emitter and absorber, respectively, and θ_e and θ_a are the polar angles the beam occupies on the emitter and absorber sides, respectively (Fig. 4). Thus, the maximum étendue that the transmitted beam can occupy is limited by the absorber side, which has a smaller area. In order to enable the most benefit from the nonreciprocity, in the nonreciprocal frequency range ΔE, we set $\theta_a = \pi/2$ such that the étendue that has the nonreciprocal functionality can be maximized. In doing so, $\theta_e = \sin^{-1}(\beta^{-1/2})$, where $\beta = A_e/A_a$ is the ratio of the emitter and the absorber areas. For the angular range of $(0, \theta_e)$, the transmissivity of the emitter is unity, and therefore the absorptivity of the emitter, α_θ, in this range is zero. For the rest of the angular range $(\theta_e, \pi/2)$, we assume the emitter has the same properties as in the reciprocal case, i.e., $\alpha_\theta = 1$.

For reciprocal STPV systems with the properties in Fig. 3(a), the temperature of the intermediate layer can be solved from the energy balance,

$$A_a E_s + A_e E_c(E_g, E_g+\Delta E, V, T_c) = A_a E_b(0,\infty,0,T_l) + A_e E_l(E_g, E_g+\Delta E, 0, T_l). \tag{9}$$

The area of the cell A_c is the same as A_e, and the cell and the emitter are close enough that the view factor between them is unity. T_c is the temperature of the cell, E_c is the energy emitted by the cell, E_b is the energy emitted from the absorber towards the sun, and E_l is the energy emitted from the intermediate layer to the cell. The energy fluxes are obtained as

$$E(E_1,E_2,V,T) = \frac{2\pi}{h^3c^2}\int_{E_1}^{E_2}\frac{E^3}{\exp((E-qV)/kT)-1}dE, \tag{10}$$

where h is the Planck constant, c is the speed of light, and k is the Boltzmann constant. T is the temperature of the emitter, E_1 and E_2 are the lower and higher energy bounds of the integration, respectively, and qV is the chemical potential of photons [39,40], where V is the voltage on the emitter. For the intermediate layer, $V = 0$, and for the cell, $V > 0$ for the above band gap part. The external quantum efficiency of the cell is assumed to be unity. In this case, the voltage and current of the cell can be obtained based on a detailed balance [1]

$$I = qA_c[N(E_g, E_g+\Delta E, 0, T_l) - N(E_g, E_g+\Delta E, V, T_c)], \tag{11}$$

where N is the photon flux obtained as

$$N(E_1,E_2,V,T) = \frac{2\pi}{h^3c^2}\int_{E_1}^{E_2}\frac{E^2}{\exp((E-qV)/kT)-1}dE. \tag{12}$$

The cell and the intermediate layer equations are coupled, and we solve the temperature of the intermediate layer and the voltage and current of the cell using an iterative approach for different area ratios. The efficiency of the STPV system is defined as $\eta = P/E_s$, where $P = IV$ is the produced electricity. For each β, we search for ΔE and E_g to find the highest efficiency. The solved efficiencies, which represent the limiting performance given by detailed balance for STPV systems with single-junction cells, are shown in the orange curve in Fig. 5. As β increases, the bandwidth of the emitter becomes narrower, and thus a higher content of emitted energy can

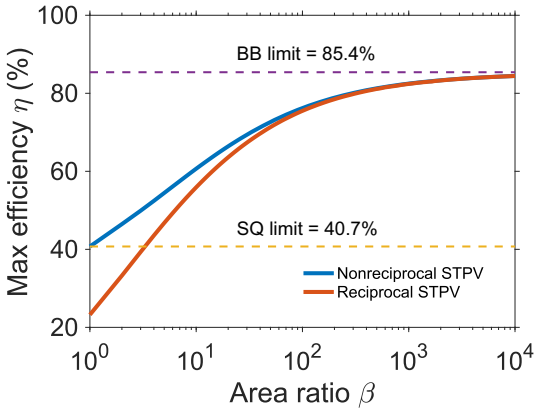

FIG. 5. Efficiency of nonreciprocal and reciprocal STPV with a single-junction cell for different area ratios β. Blue and orange curves show the efficiencies of NSTPVs and reciprocal STPVs, respectively. The Shockley-Queisser limit and the blackbody limit are independent of β. They are marked as horizontal dashed lines in the figure.

be converted to electricity, yielding a higher efficiency. The efficiency surpasses the SQ limit when β is larger than about 3, indicating a minimum required area ratio for single-junction STPV to outperform the SQ limit. The band gaps and ΔE at different β are provided in Appendix A.

As noted previously, an infinitely large area ratio is needed to reach the ultimate efficiency. This can be readily shown with the above equations. In this case, ΔE approaches zero, the photon fluxes can be obtained as

$$N_e = \frac{2\pi}{h^3c^2}\frac{E_g^2}{\exp(E_g/kT_l)-1}\delta E \tag{13}$$

and

$$N_c = \frac{2\pi}{h^3c^2}\frac{E_g^2}{\exp((E_g-qV)/kT_c)-1}\delta E. \tag{14}$$

Here, N_e and N_c are the photon fluxes from the emitter and the cell, respectively. The efficiency of the converter can be defined as $\eta_{\mathrm{PV}} = W/Q$, where $W = qV(N_e - N_c)$ and $Q = E_g(N_e - N_c)$. Therefore, in this limiting case

$$\eta_{\mathrm{PV}} = \frac{qV}{E_g}. \tag{15}$$

The highest efficiency happens when the voltage is approaching the highest value, which is the open-circuit voltage (V_{OC}) obtained by setting $I = 0$ in Eq. (11)

$$\frac{E_g}{kT_l} = \frac{E_g - qV_{\mathrm{OC}}}{kT_c}. \tag{16}$$

Combining Eqs. (15) and (16), one obtains $\eta_{PV} = 1 - (T_c/T_l)$, indicating that the cell is a Carnot convertor in the monochromatic limit. Since the absorber is essentially a blackbody in this case, the overall efficiency is shown as Eq. (4), yielding 85.4% at $T_l = 2544$ K, the blackbody limit.

Now we consider the nonreciprocal STPV with an intermediate layer that possesses radiative properties depicted in Fig. 3(b). Compared to the reciprocal STPV, the detailed balance and the efficiency calculation for the cell are the same. The only difference is in the energy balance for the intermediate layer,

$$\begin{aligned} &A_aE_s + \alpha A_eE_c(E_g, E_g+\Delta E, V, T_c) \\ &\quad = A_aE_b(0, E_g, 0, T_l) + A_aE_b(E_g+\Delta E, \infty, 0, T_l) \\ &\qquad + A_eE_l(E_g, E_g+\Delta E, 0, T_l), \end{aligned} \tag{17}$$

where

$$\alpha = \frac{\int_0^{2\pi}\int_0^{\pi/2}\alpha_\theta\cos\theta\,\sin\theta\,d\theta\,d\phi}{\int_0^{2\pi}\int_0^{\pi/2}\cos\theta\,\sin\theta\,d\theta\,d\phi} = 1-\sin^2\theta_e \tag{18}$$

is the hemispherical absorptivity of the emitter in the nonreciprocal frequency range ΔE. In the nonreciprocal system, the étendue of the transmitted emission from the cell through the intermediate layer (the lost energy as compared with the reciprocal system) is the same as the étendue of the suppressed radiation from the intermediate layer towards the sun (the suppressed energy loss as compared with the reciprocal system). Since the intensity of emission from the intermediate layer is always higher than that from the cell, the nonreciprocal functionality allows a higher energy flux to the NSTPV system and a higher temperature of the nonreciprocal intermediate layer compared with the reciprocal STPV system. Thus, the efficiency of the NSTPV is always higher than that of the STPV, as shown in Fig. 5, indicating the significant benefits and effectiveness of NSTPVs.

For $\beta = 1$, Eq. (17) yields $T_l = T_s$ regardless of the choice of ΔE. Such a scenario resembles the case when the sun directly illuminates the cell. Therefore, the maximum power production happens when the incoming photon flux is maximized, i.e., $\Delta E = \infty$, and the efficiency equals the SQ limit. Therefore, the nonreciprocal layer does not bring additional benefits for $\beta = 1$ compared with a single cell directly exposed to the sunlight. However, for $\beta > 1$, the efficiency increases for the same reason as the reciprocal STPV. Therefore, the NSTPV systems can outperform the SQ limit for all area ratios higher than 1. For small β, the optimized ΔE is relatively large. In this case, the suppressed radiated energy from the absorber is much stronger than the emission from the cell and consequently the nonreciprocal system has much higher efficiency than the reciprocal system (Fig. 5). As β increases, the optimized ΔE becomes smaller and the temperature of the

intermediate layer also decreases (see Appendix B). Therefore, the benefits of the suppressed back emission due to nonreciprocity become weaker. In fact, in the limiting case with an infinitely large area ratio, $\theta_e \approx 0$, ΔE becomes infinitesimal. Thus, the energy balance equation of the nonreciprocal system will approach the reciprocal system, resulting in the same limit for both systems.

We note that, as has been discussed and realized in existing literature and designs, a large area ratio can induce several critical issues and is not favored in practice. For example, a large β causes larger thermal resistance from the absorber to the emitter, inefficient cooling of the cell, and significant energy loss due to convection from the intermediate layer. Thus, the suggested area ratios for STPVs, as discussed in existing studies [30,41–45], are about 10, which falls in the region where the efficiencies of NSTPVs are much higher than STPVs. Therefore, the proposed NSTPV system represents a pathway to significantly improve the performance of STPV systems in practice. In Appendix A, we provide the band gaps and the bandwidth of the reciprocal and nonreciprocal STPVs at optimal operation points for different β.

As final remarks, we discuss some practical aspects regarding the proposed NSTPV system. In this study, we focus on fully concentrated light and neglect the nonradiative recombination effect to obtain the limiting performance of the nonreciprocal system. The benefit of the nonreciprocity still holds for the other concentration factors and practical cells with nonradiative nonidealities, and the efficiency can be analyzed following the same procedure we present in this study by modifying the detailed balance equations. For the nonreciprocal intermediate layer, nonreciprocity for both polarizations are required. The design in Ref. [21] is a one-dimensional photonic crystal structure, which is designed for transverse-magnetic waves only, and it can be expanded to two-dimensional structures to provide the nonreciprocal functionalities needed for both polarizations. One can also separate the two polarizations using a polarization splitter to direct the two polarizations to two separate systems that are respectively optimized for one polarization. Our work also points to the important application of high-temperature stable nonreciprocal thermal emitters. Recent studies on magneto-optical materials [17,18,46] and magnetic Weyl semimetals [20,47–50] demonstrate promising pathways to achieve these proposed radiative properties. Alternatively, as indicated in Fig. 2(a), one may separate the nonreciprocal circulation functionality from the absorbing and reemitting functionality. In this way, the circulator can be designed to be a low-loss component using nonreciprocal material, and therefore there will be no need for it to be high-temperature endurable. The blackbody components will need to be stable at high temperatures, and various practical materials can be used to achieve this [51]. Our system also reveals the necessity of broadband nonreciprocal behavior. Recent works [52,53] offer valuable insights on achieving broadband nonreciprocity.

III. CONCLUSION

To summarize, we propose a NSTPV system with the intermediate layer possessing nonreciprocal radiative properties. We show that the system approaches the Landsberg limit in the ideal case. With a wavelength-selective nonreciprocal intermediate layer, we observe significant improvement in practical STPV systems with single-junction cells as compared with the traditional reciprocal STPV systems. Here we focus on systems with planar intermediate layers. Other geometries, such as a cylindrical shape [30], can also be used to allow more compact systems. Similarly, the adaption of the nonreciprocal intermediate layer should also bring significant benefit to STPVs using multijunction photovoltaic cells or other photonic heat engines. Our work highlights the great potential of nonreciprocal thermal photonic components in energy applications. The proposed system offers an alternative pathway to improve the performance of STPV systems significantly. It may pave the way for nonreciprocal systems to be implemented in practical STPV systems currently used in power plants.

ACKNOWLEDGMENTS

B.Z. acknowledges the start-up funding from the University of Houston. The authors are grateful for the support of the Research Computing Data Core at the University of Houston for assistance with the calculations carried out in this work.

The authors declare no competing financial interest.

TABLE I. The properties of the nonreciprocal STPV system at optimal operation points for each area ratio.

Area ratio β	Band gap of the cell E_g (eV)	Bandwidth of the emitter ΔE (eV)
1	1.11	∞
2	1.177	3.513
3	1.208	2.12
4	1.223	1.626
5	1.231	1.367
10	1.224	0.806
15	1.21	0.618
25	1.192	0.446
50	1.166	0.292
100	1.131	0.193
200	1.105	0.129
300	1.097	0.104
500	1.097	0.079
800	1.071	0.06
1500	1.097	0.045
3000	1.062	0.03

TABLE II. The properties of the reciprocal STPV system at optimal operation points for each area ratio.

Area ratio β	Band gap of the cell E_g (eV)	Bandwidth of the emitter ΔE (eV)
1	1.177	3.513
2	1.208	2.130
3	1.223	1.626
4	1.231	1.348
5	1.232	1.168
10	1.223	0.756
15	1.208	0.594
25	1.192	0.432
50	1.157	0.287
100	1.14	0.193
200	1.114	0.129
300	1.105	0.104
500	1.097	0.079
800	1.071	0.06
1500	1.097	0.045
3000	1.062	0.03

APPENDIX A: PROPERTIES OF THE SYSTEM AT OPTIMIZED OPERATION POINTS

Tables I and II are the properties of the nonreciprocal and reciprocal STPV systems at the optimal operation points for different area ratios, respectively.

APPENDIX B: TEMPERATURE OF THE INTERMEDIATE LAYER

Figure 6 shows the solved temperature of the intermediate layer at each area ratio up to 20. We show the temperature in this area ratio range because the best performance of nonreciprocal STPVs compared with reciprocal STPVs, and also the applicable area ratios that have been studied in practice are within this range. The blue curve corresponds to the nonreciprocal, and the orange curve corresponds to the reciprocal intermediate layer. As the area ratio increases, the operation temperature of the intermediate layer decreases, with the nonreciprocal case and the reciprocal case approaching each other.

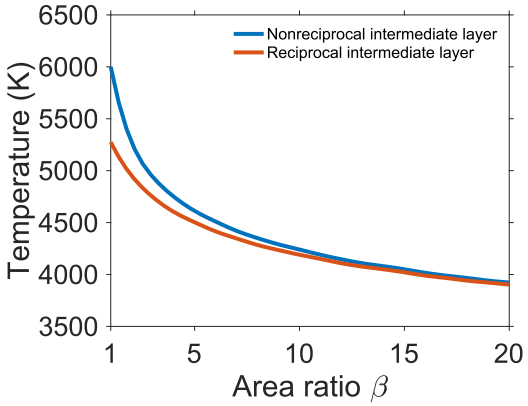

FIG. 6. Temperature of the intermediate layer in reciprocal and nonreciprocal STPV at each area ratio.

[1] W. Shockley and H. J. Queisser, Detailed balance limit of efficiency of p-n junction solar cells, J. Appl. Phys. **32**, 510 (1961).
[2] M. A. Green, in *Third Generation Photovoltaics* (Springer Berlin, Heidelberg, 2006), Vol. 12. PHOTONICS.
[3] D. L. Chubb, B. S. Good, and R. A. Lowe, in *AIP Conf. Proc.* (American Institute of Physics, New York, 1996), pp. 181–198.
[4] A. Datas, D. L. Chubb, and A. Veeraragavan, Steady state analysis of a storage integrated solar thermophotovoltaic (SISTPV) system, Sol. Energy **96**, 33 (2013).
[5] C. Amy, H. R. Seyf, M. A. Steiner, D. J. Friedman, and A. Henry, Thermal energy grid storage using multi-junction photovoltaics, Energy Environ. Sci. **12**, 334 (2019).
[6] H. R. Seyf and A. Henry, Thermophotovoltaics: a potential pathway to high efficiency concentrated solar power, Energy Environ. Sci. **9**, 2654 (2016).
[7] A. LaPotin, K. L. Schulte, M. A. Steiner, K. Buznitsky, C. C. Kelsall, D. J. Friedman, E. J. Tervo, R. M. France, M. R. Young, A. Rohskopf, *et al.*, Thermophotovoltaic efficiency of 40%, Nature **604**, 287 (2022).
[8] W. Chan, R. Huang, C. Wang, J. Kassakian, J. Joannopoulos, and I. Celanovic, Modeling low-bandgap thermophotovoltaic diodes for high-efficiency portable power generators, Sol. Energy Mater. Sol. Cells **94**, 509 (2010).
[9] W. R. Chan, P. Bermel, R. C. Pilawa-Podgurski, C. H. Marton, K. F. Jensen, J. J. Senkevich, J. D. Joannopoulos, M. Soljačić, and I. Celanovic, Toward high-energy-density, high-efficiency, and moderate-temperature chip-scale thermophotovoltaics, Proc. Natl. Acad. Sci. U. S. A. **110**, 5309 (2013).
[10] A. Datas and A. Martí, Thermophotovoltaic energy in space applications: Review and future potential, Sol. Energy Mater. Sol. Cells **161**, 285 (2017).
[11] G. Kirchhoff, in *Von Kirchhoff bis Planck* (Springer, Wiesbaden, 1978), pp. 131–151.
[12] D. G. Baranov, Y. Xiao, I. A. Nechepurenko, A. Krasnok, A. Alù, and M. A. Kats, Nanophotonic engineering of far-field thermal emitters, Nat. Mater. **18**, 920 (2019).
[13] S. Fan, Thermal photonics and energy applications, Joule **1**, 264 (2017).
[14] V. Rinnerbauer, A. Lenert, D. M. Bierman, Y. X. Yeng, W. R. Chan, R. D. Geil, J. J. Senkevich, J. D. Joannopoulos, E. N. Wang, M. Soljačić, *et al.*, Metallic photonic crystal absorber-emitter for efficient spectral control in high-temperature solar thermophotovoltaics, Adv. Energy Mater. **4**, 1400334 (2014).
[15] Y. Wang, L. Zhou, Q. Zheng, H. Lu, Q. Gan, Z. Yu, and J. Zhu, Spectrally selective solar absorber with sharp and temperature dependent cut-off based on semiconductor nanowire arrays, Appl. Phys. Lett. **110**, 201108 (2017).
[16] Y. Wang, H. Liu, and J. Zhu, Solar thermophotovoltaics: Progress, challenges, and opportunities, APL Mater. **7**, 080906 (2019).

[17] L. Zhu and S. Fan, Near-Complete Violation of Detailed Balance in Thermal Radiation, Phys. Rev. B **90**, 220301 (2014).

[18] B. Zhao, Y. Shi, J. Wang, Z. Zhao, N. Zhao, and S. Fan, Near-complete violation of Kirchhoff's law of thermal radiation with a 0.3 T magnetic field, Opt. Lett. **44**, 4203 (2019).

[19] Y. Tsurimaki, X. Qian, S. Pajovic, F. Han, M. Li, and G. Chen, Large Nonreciprocal Absorption and Emission of Radiation in Type-I Weyl Semimetals with Time Reversal Symmetry Breaking, Phys. Rev. B **101**, 165426 (2020).

[20] B. Zhao, C. Guo, C. A. Garcia, P. Narang, and S. Fan, Axion-field-enabled nonreciprocal thermal radiation in Weyl semimetals, Nano Lett. **20**, 1923 (2020).

[21] Y. Park, V. S. Asadchy, B. Zhao, C. Guo, J. Wang, and S. Fan, Violating Kirchhoff's law of thermal radiation in semitransparent structures, ACS Photonics **8**, 2417 (2021).

[22] P. Landsberg and G. Tonge, Thermodynamic energy conversion efficiencies, J. Appl. Phys. **51**, R1 (1980).

[23] M. A. Green, Time-asymmetric photovoltaics, Nano Lett. **12**, 5985 (2012).

[24] Y. Park, B. Zhao, and S. Fan, Reaching the ultimate efficiency of solar energy harvesting with a nonreciprocal multijunction solar cell, Nano Lett. **22**, 448 (2021).

[25] M. Planck, *The Theory of Heat Radiation* (Blakiston, Philadelphia, 1914).

[26] A. De Vos and H. Pauwels, Comment on a thermodynamical paradox presented by P. Wurfel, J. Phys. C: Solid State Phys. **16**, 6897 (1983).

[27] L. Zhu and S. Fan, Persistent Directional Current at Equilibrium in Nonreciprocal Many-Body Near Field Electromagnetic Heat Transfer, Phys. Rev. Lett. **117**, 134303 (2016).

[28] N.-P. Harder and P. Würfel, Theoretical limits of thermophotovoltaic solar energy conversion, Semicond. Sci. Technol. **18**, S151 (2003).

[29] T. Burger, C. Sempere, B. Roy-Layinde, and A. Lenert, Present efficiencies and future opportunities in thermophotovoltaics, Joule **4**, 1660 (2020).

[30] E. Rephaeli and S. Fan, Absorber and emitter for solar thermo-photovoltaic systems to achieve efficiency exceeding the Shockley-Queisser limit, Opt. Express **17**, 15145 (2009).

[31] D. M. Bierman, A. Lenert, W. R. Chan, B. Bhatia, I. Celanović, M. Soljačić, and E. N. Wang, Enhanced photovoltaic energy conversion using thermally based spectral shaping, Nat. Energy **1**, 1 (2016).

[32] W. Spirkl and H. Ries, Solar thermophotovoltaics: an assessment, J. Appl. Phys. **57**, 4409 (1985).

[33] Z. Zhou, E. Sakr, Y. Sun, and P. Bermel, Solar thermophotovoltaics: reshaping the solar spectrum, Nanophotonics **5**, 1 (2016).

[34] Z. Omair, G. Scranton, L. M. Pazos-Outón, T. P. Xiao, M. A. Steiner, V. Ganapatim, P. F. Peterson, J. Holzrichter, H. Atwater, and E. Yablonovitch, Ultraefficient thermophotovoltaic power conversion by band-edge spectral filtering, Proc. Natl. Acad. Sci. U. S. A. **116**, 15356 (2019).

[35] D. Fan, T. Burger, S. McSherry, B. Lee, A. Lenert, and S. R. Forrest, Near-perfect photon utilization in an air-bridge thermophotovoltaic cell, Nature **586**, 237 (2020).

[36] H. Zhang, C. W. Hsu, and O. D. Miller, Scattering concentration bounds: Brightness theorems for waves, Optica **6**, 1321 (2019).

[37] D. A. Miller, Waves, modes, communications, and optics: a tutorial, Adv. Opt. Photonics **11**, 679 (2019).

[38] J. Chaves, *Introduction to nonimaging optics* (CRC Press, Boca Raton, 2008).

[39] P. Wurfel, The chemical potential of radiation, J. Phys. C: Solid State Phys. **15**, 3967 (1982).

[40] B. Zhao and S. Fan, Chemical potential of photons and its implications for controlling radiative heat transfer, Annu. Rev. Heat Transfer **23**, 397 (2020).

[41] A. Lenert, D. M. Bierman, Y. Nam, W. R. Chan, I. Celanović, M. Soljačić, and E. N. Wang, A nanophotonic solar thermophotovoltaic device, Nat. Nanotechnol. **9**, 126 (2014).

[42] C. Ungaro, S. K. Gray, and M. C. Gupta, Solar thermophotovoltaic system using nanostructures, Opt. Express **23**, A1149 (2015).

[43] A. Kohiyama, M. Shimizu, and H. Yugami, Unidirectional radiative heat transfer with a spectrally selective planar absorber/emitter for high-efficiency solar thermophotovoltaic systems, Appl. Phys. Express **9**, 112302 (2016).

[44] R. Bhatt, I. Kravchenko, and M. Gupta, High-efficiency solar thermophotovoltaic system using a nanostructure-based selective emitter, Sol. Energy **197**, 538 (2020).

[45] R. Bhatt and M. Gupta, Design and validation of a high-efficiency planar solar thermophotovoltaic system using a spectrally selective emitter, Opt. Express **28**, 21869 (2020).

[46] K. J. Shayegan, B. Zhao, Y. Kim, S. Fan, and H. A. Atwater, Nonreciprocal infrared absorption via resonant magneto-optical coupling to InAs, Sci. Adv. **8**, eabm4308 (2022).

[47] D. Liu, A. Liang, E. Liu, Q. Xu, Y. Li, C. Chen, D. Pei, W. Shi, S. Mo, P. Dudin, *et al.*, Magnetic Weyl semimetal phase in a Kagomé crystal, Science **365**, 1282 (2019).

[48] N. Morali, R. Batabyal, P. K. Nag, E. Liu, Q. Xu, Y. Sun, B. Yan, C. Felser, N. Avraham, H. Beidenkopf, *et al.*, Fermi-arc diversity on surface terminations of the magnetic Weyl semimetal $Co_3Sn_2S_2$, Science **365**, 1286 (2019).

[49] I. Belopolski, K. Manna, D. S. Sanchez1, G. Chang, B. Ernst, J. Yin, S. S. Zhang, T. Cochran, N. Shumiya, H. Zheng, *et al.*, Discovery of topological Weyl fermion lines and drumhead surface states in a room temperature magnet, Science **365**, 1278 (2019).

[50] H. Tsai, T. Higo, K. Kondou, T. Nomoto, A. Sakai, A. Kobayashi, T. Nakano, K. Yakushiji, R. Arita, S. Miwa, *et al.*, Electrical manipulation of a topological antiferromagnetic state, Nature **580**, 608 (2020).

[51] X. Wang, R. Starko-Bowes, C. Khandekar, and Z. Jacob, High-temperature thermal photonics, Annu. Rev. Heat Transfer **23**, 355 (2020).

[52] M. Liu, S. Xia, W. Wan, J. Qin, H. Li, C. Zhao, L. Bi, and C.-W. Qiu, Nonreciprocal thermal radiation in ultrathin magnetized epsilon-near-zero semiconductors, arXiv preprint arXiv:2203.04488 (2022).

[53] J. Wu, F. Wu, T. Zhao, M. Antezza, and X. Wu, Dual-band nonreciprocal thermal radiation by coupling optical Tamm states in magnetophotonic multilayers, Int. J. Therm. Sci. **175**, 107457 (2022).